Journal of Sound and Vibration (2000) **235**(3), 451–476
doi:10.1006/jsvi.2000.2929, available online at http://www.idealibrary.com on IDEAL®

A MODAL INTERACTION INDICATOR FOR QUALIFYING Cs AS AN INDICATOR OF STRENGTH OF COUPLING BETWEEN SEA SUBSYSTEMS

P. P. JAMES

SEP division de SNECMA, 27200, *Vernon, France*

AND

F. J. FAHY

*Institute of Sound and Vibration Research, University of Southampton, Southampton SO*17 1*BJ*, *England*

(*Received* 15 *March* 1999, *and in final form* 8 *February* 2000)

In two previous papers [1, 2], a technique for the indication of strength of coupling between SEA subsystems was proposed. However, an apparent limitation to the use of the coupling strength indicator C_S was revealed by computational simulation. Whereas a value for C_S greater than 0·07 clearly indicates weak coupling, a smaller value only confirms strong coupling between subsystems when the uncoupled resonance frequencies of each subsystem are sufficiently proximate. In order to overcome this major difficulty in the interpretation of small values for C_S, an indicator of modal interaction M_p is proposed. In the case of weak coupling, modal interaction is directly related to the proximity between uncoupled resonance frequencies. The definition of M_p relies upon both a deterministic analysis of the coupling between two oscillators and a statistical model of interaction between uncoupled resonant modes. M_p can be assessed on assembled structures and improves the reliability of C_S as an indicator of strength of coupling between SEA subsystems.

1. INTRODUCTION

An indicator of strength of coupling in a SEA sense, denoted by C_S, has been proposed in references [1, 2]. Two subsystems should be considered as weakly coupled in a SEA sense only when values obtained for C_S are greater than 0·07. This indicator appears to be "user-friendly" and provides the experimenter with a rapid assessment of strength of coupling between assumed statistical energy analysis subsystems of an assembled structure within a frequency band. However, although they are not apparent from the experimental results presented in reference [2], some restrictions on the practical usefulness of C_S have been suggested by theoretical studies presented in reference [1]. C_S appears to be very sensitive to the frequency separation between the modal frequencies of each uncoupled subsystem and can yield values less than 0·07 even in the case of weak coupling. In fact, this occurs when there is no interaction between modes localized on each subsystems [3]. *Modal interaction* is then defined as a state where the modal frequencies of each subsystem are sufficiently proximate within a frequency band to produce values of C_S greater than 0·07 in all cases of weak coupling. The reliability of C_S as an indicator of strength of coupling in a SEA sense depends highly on this modal interaction. If C_S is less than 0·07, then *either* the

0022-460X/00/330451 + 26 $35.00/0

two subsystems are weakly coupled, but without modal interaction, *or* they are strongly coupled. If C_S is greater than 0·07, then the two subsystems considered are weakly coupled in a SEA sense. It is only when C_S is less than 0·07 that its reliability is questioned. The experimenter has to decide if the assumed SEA subsystems are weakly coupled, but with no modal interaction, or if they are, in fact, strongly coupled. This work aims at providing the experimenter with an indicator of modal interaction.

First, the definition of C_S is briefly presented and one example of its sensitivity to frequency separation is provided. Then, for two coupled oscillators, the sensitivity of C_S to the relative location of their two resonance frequencies is studied by means of numerical tests for a wide range of strength of coupling. In the case of very weak coupling, C_S is derived as a function both of natural frequencies and their modal dampings. Finally, based upon all these results, an indicator of probability of modal interaction is proposed. It is denoted by M_p and can be used on any subsystem provided its modal density and internal loss factor are known. M_p forms a basis for distinguishing between (i) weak coupling without modal interaction and (ii) strong coupling.

It should be noticed that the M_p definition relies upon studies of one-dimensional systems. Although it is very sensitive to resonance frequency matching, M_p does not take into account matching in the space domain between mode shapes. The problem of mode shape matching poses a limitation to M_p, the significance of which requires further investigation.

2. A BRIEF DESCRIPTION OF C_S

In references [1, 2] an indicator related to Langley's definition of weak coupling in a SEA sense [4] has been developed in the time domain. This indicator is based on the time delays to the peaks of the envelope of the band-pass-filtered local kinetic energies in the subsystems when one subsystem is subjected to a force impulse. It appears that the shape of the temporal moving average (or envelope) of the band-pass-filtered kinetic energy of the indirectly excited subsystem can be related to the strength of coupling. In the case of weak coupling, there is an appreciable time delay to the peak of the band-pass-filtered kinetic energy of the indirectly excited subsystem, as shown by the case of two spring-coupled rods carrying longitudinal waves (Figure 1).

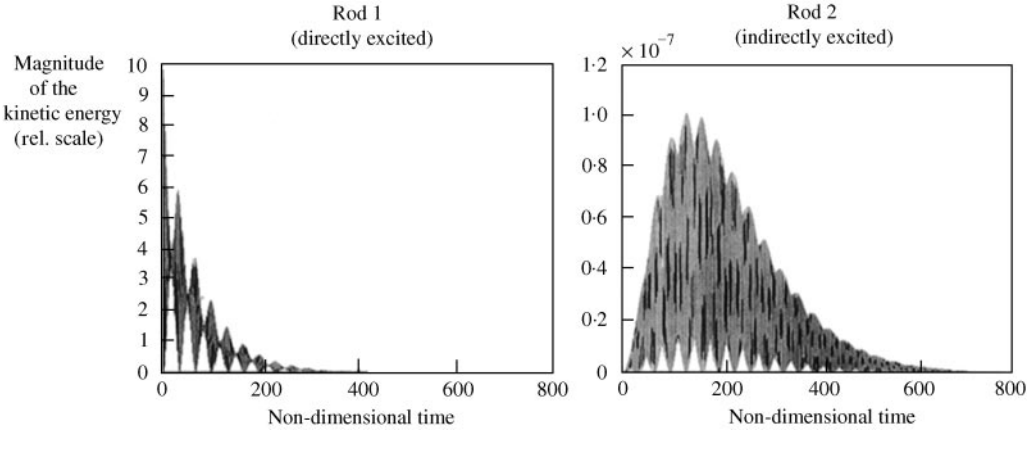

Figure 1. Temporal evolution of the kinetic energy of two weakly coupled rods when subject to an impulse force.

When the strength of coupling is increased, the response of the indirectly excited rod tends towards the response of the directly excited rod. The particular patterns of these responses to impulse excitation lead to the proposal of a general, non-dimensional indicator of the coupling strength in an SEA sense based upon the temporal moving average of kinetic energy (Figure 2). The indicator of coupling strength is denoted by C_S. For all the systems considered, the range of values obtained for C_S is always the same [1, 2]. This suggests that C_S is an absolute indicator of the strength of coupling independent of the system considered.

All the results presented in references [1, 2] have led to the choice of a threshold of $C_S = 0{\cdot}07$ above which the coupled subsystems can be considered as weakly coupled in a SEA sense. However, theoretical studies have shown that C_S is sensitive to the degree of proximity of resonance frequencies of the uncoupled modes of the subsystems [1]. This phenomenon could induce a misinterpretation of the indication provided by C_S. In the case of weak coupling, if the uncoupled resonance frequencies are not proximate enough, the value obtained for C_S is very small (Figure 3). Therefore, the experimenter would wrongly conclude that the two subsystems considered are strongly coupled. The aim of the following sections is to propose a way to overcome this apparently restrictive condition for a practical use of C_S.

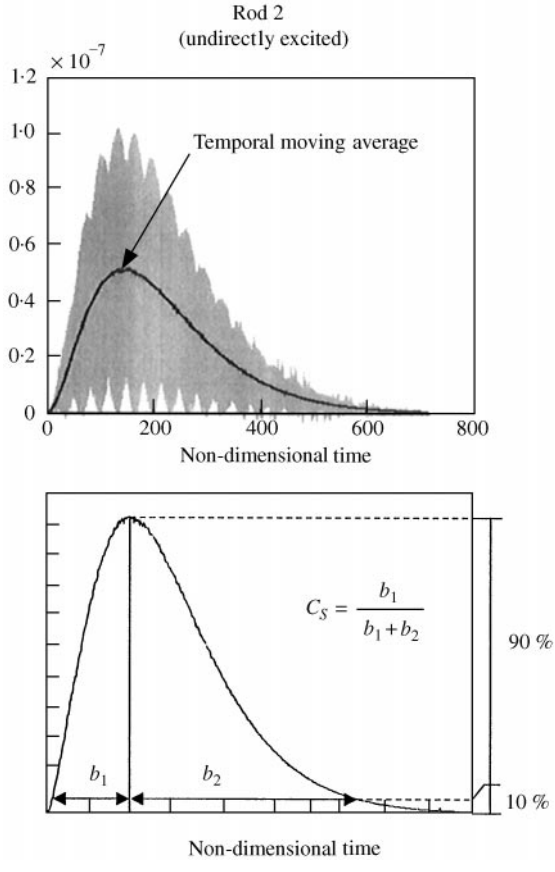

Figure 2. Definition of a non-dimensional measure of the strength of coupling C_S.

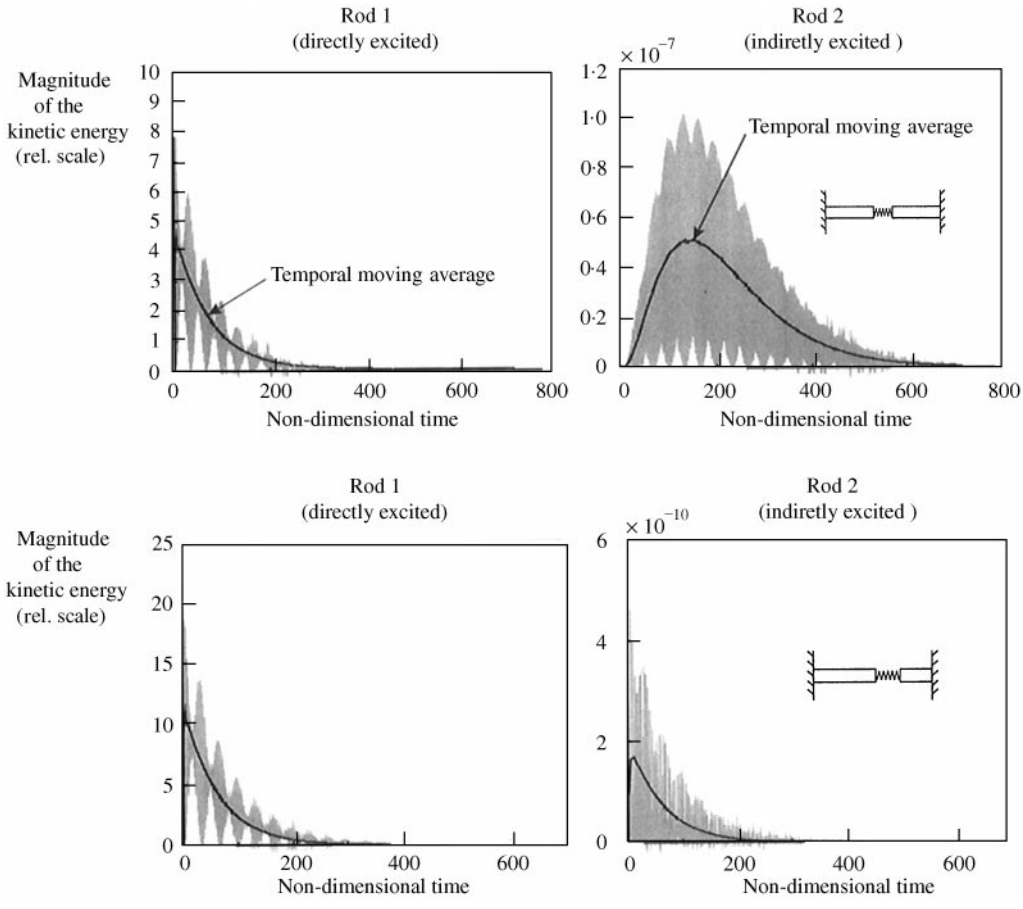

Figure 3. Sensitivity of C_S to proximity between uncoupled resonance frequencies. Case 1: the two rods are similar, the uncoupled resonance frequencies are the same for both subsystems. Case 2: the length of rod 2 is half the length of rod 1. The uncoupled resonance frequencies are not the same in the frequency band considered.

3. THE CASE OF TWO COUPLED OSCILLATORS AND ARBITRARY STRENGTH OF COUPLING

3.1. DESCRIPTION OF THE SYSTEM

The system studied in this section consists of two oscillators coupled by a spring. The coupling is assumed to be conservative. The masses and viscous damping of both oscillators are the same (Figure 4). The only varied parameters are K_2, the spring stiffness of oscillators 2, and k, the stiffness of the coupling spring. This is not too restrictive insofar as the main purpose of this section is to study C_S as a function of uncoupled resonance frequencies and strength of coupling. Modal proximity between the uncoupled resonance frequencies is directly related to the value of K_2, whereas "strength" of coupling is proportional to k.

In order to derive C_S, the system is subject to an impulse force and the velocity response of the indirectly excited oscillator is analyzed. The dynamics of the system in Figure 4 are expressed by

$$\begin{aligned} m\ddot{x}_1 + K_1 x_1 + k(x_1 - x_2) + \mathrm{d}\dot{x}_1 &= I\delta(t), \\ m\ddot{x}_2 + K_2 x_2 + k(x_2 - x_1) + \mathrm{d}\dot{x}_2 &= 0, \end{aligned} \tag{1}$$

where x_1 and x_2 are the displacements of masses m and I is the magnitude of the impulse force.

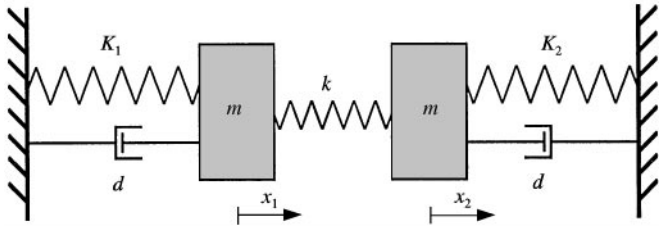

Figure 4. Two coupled oscillators with conservative coupling.

In the frequency domain, the Fourier transform of equation (1) may be written

$$-\omega^2\begin{bmatrix} m & 0 \\ 0 & m \end{bmatrix}\begin{bmatrix} \tilde{X}_1 \\ \tilde{X}_2 \end{bmatrix}+\begin{bmatrix} K_1+k & -k \\ -k & K_2+k \end{bmatrix}\begin{bmatrix} \tilde{X}_1 \\ \tilde{X}_2 \end{bmatrix}+\mathrm{i}\omega\begin{bmatrix} d & 0 \\ 0 & d \end{bmatrix}\begin{bmatrix} \tilde{X}_1 \\ \tilde{X}_2 \end{bmatrix}=\begin{bmatrix} I \\ 0 \end{bmatrix}, \tag{2}$$

where $\tilde{X}_1$ and $\tilde{X}_2$ are the Fourier transforms of displacements $x_1(t)$ and $x_2(t)$. Equation (2) yields

$$\begin{aligned} \tilde{X}_1 &= \frac{-m\omega^2+K_2+k+\mathrm{i}d\omega}{[(-m\omega^2+K_1+k+\mathrm{i}d\omega)(-m\omega^2+K_2+k+\mathrm{i}d\omega)-k^2]}\,I, \\ \tilde{X}_2 &= \frac{k}{[(-m\omega^2+K_1+k+\mathrm{i}d\omega)(-m\omega^2+K_2+k+\mathrm{i}d\omega)-k^2]}\,I. \end{aligned} \tag{3}$$

The uncoupled resonance frequencies are

$$\omega_1^d=\sqrt{\frac{K1}{m}}\sqrt{1-\frac{1}{4}\eta_1^2} \quad \text{and} \quad \omega_2^d=\sqrt{\frac{K_2}{m}}\sqrt{1-\frac{1}{4}\eta_2^2}, \tag{4}$$

where $\eta_1=\mathrm{d}/\sqrt{K_1\ m}$ and $\eta_2=\mathrm{d}/\sqrt{K_2 m}$ are loss factors, equal to twice and damping ratios

For both oscillators, masses and spring stiffness have been arbitrarily chosen, insofar as, according to reference [5], C_S is sensitive to the relative separation between the resonance frequencies but not to their absolute value. The viscous damping coefficients have been chosen in order to yield reasonable values for the loss factors. The selected physical characteristics of the system are presented in Table 1.

Unlike η_2 and ω_2^d, the modal bandwidth $\eta_2\omega_2$ does not depend on K_2 for $\eta_2\omega_2=d/m$ with $\omega_2=\sqrt{K_2/m}$. The resonance frequency ratio, r, may be expressed as a function of K_2 (Figure 5),

$$r=\frac{\omega_2^d}{\omega_1^d}=\frac{1}{\omega_1^J}\sqrt{\frac{K_2}{m}-\frac{1}{4}\left(\frac{d}{m}\right)^2}. \tag{5}$$

Preliminary tests were performed in order to choose the range of coupling stiffness for k. In case of perfect modal coincidence, for values of k between 10^{-2} and 10^5, C_S varies between 0·35 and 0. It is considered therefore that all the cases of strength of coupling have been simulated. In addition, in case of very weak coupling, the resonance frequency ratio has been varied from 0·90 to 1·1 in order to produce values of C_S varying from close to 0 to 0·35. This range of resonance frequency ratio enables us to study any strength of coupling with or without modal interaction.

TABLE 1

Physical characteristics of the coupled oscillators

Oscillator 1					Oscillator 2			Coupling
m	K_1	d	ω_1^d	η_1	m	K_2	d	k
0·1 kg	10^5 N/M	0·5 Ns/m	$\cong 10^3$ rad/s	5×10^{-3}	0·1 kg	Variable	0·5 Ns/m	Variable

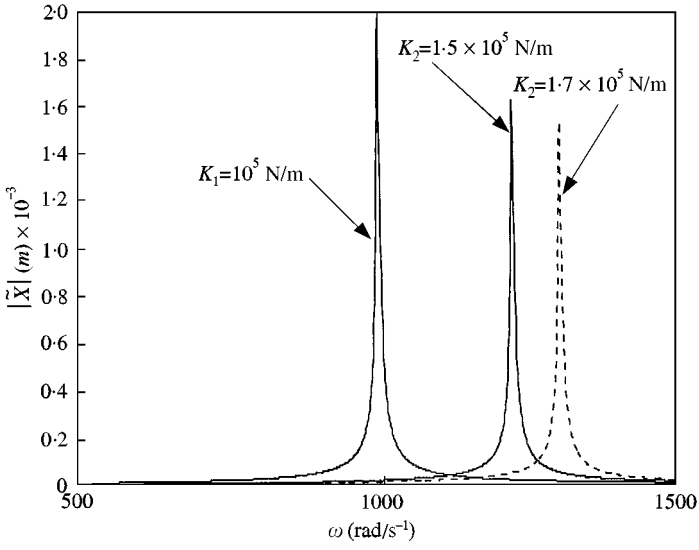

Figure 5. Example of the frequency separation between the uncoupled resonance frequencies of the oscillators as a function of K_2.

The value of d has been chosen such that η_2 lies between 10^{-3} and 10^{-2}. The velocities of masses m are derived in the time domain and squared. Subsequently, C_S is derived for various k and K_2. The results are presented in the next section.

3.2. C_S AS A FUNCTION OF THE STRENGTH OF COUPLING AND RESONANCE FREQUENCY RATIOS

On the basis of the theoretical model of two coupled oscillators described in the previous section, C_S has been derived for a range of resonance frequency ratios, coupling strength and damping (Figures 6 and 7). In order to vary the damping, d has been changed. For Figure 6, $d = 0{\cdot}1$, whereas in Figure 7, $d = 0{\cdot}01$. This yields respectively $\eta_1 = 10^{-3}$ and 10^{-2}. Unlike η_1, η_2 depends on K_2 and therefore on the resonance frequency ratios, r. Nevertheless, oscillators 1 and 2 have the same modal bandwidth and η_2 always lies between 10^{-3} and 10^{-2}.

For these two coupled oscillators, the modal overlap my be defined by

$$m = \frac{\eta_1 \omega_1}{\omega_2^d - \omega_1^d} = \frac{\eta_1 \omega_1}{\omega_1^d (1 - r)} \quad \text{with } \eta_1 \omega_1 = \eta_2 \omega_2.$$

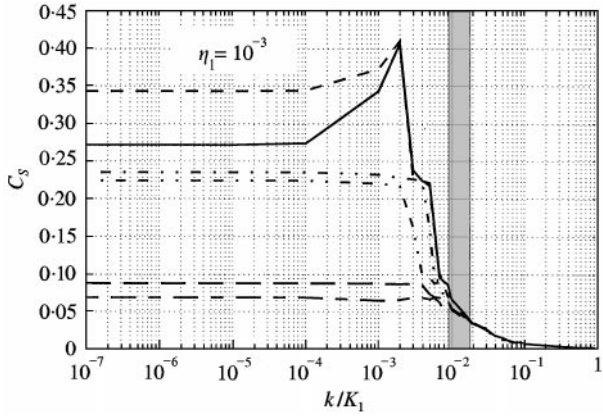

Figure 6. C_S as a function of coupling strength and resonance frequency ratio with $\eta_1 = 10^{-3}$. ——, $r = 1$; – – –, $r = 0{\cdot}999$, $m = 1$; · · – · ·, $r = 0{\cdot}997$, $m = 0{\cdot}34$; · – – –, $r = 0{\cdot}995$, $m = 0{\cdot}20$; — —, $r = 0{\cdot}992$, $m = 0{\cdot}12$; — – —, $r = 0{\cdot}990$, $m = 0{\cdot}10$.

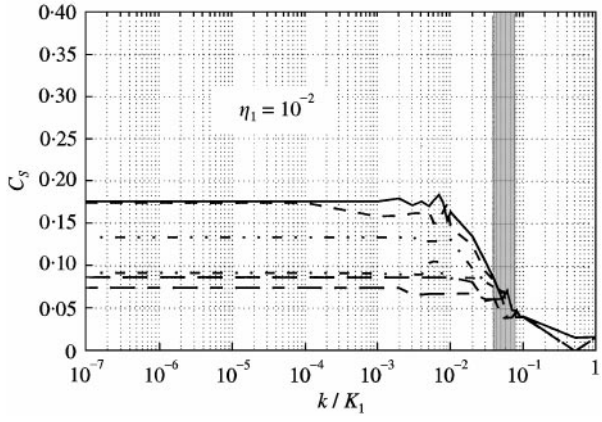

Figure 7. C_S as a function of coupling strength and resonance frequency ratio with $\eta_1 = 10^{-2}$. ——, $r = 1$; – – –, $r = 0{\cdot}999$, $m = 1$; · · · – · · ·, $r = 0{\cdot}98$, $m = 0{\cdot}50$; · – – –, $r = 0{\cdot}97$, $m = 0{\cdot}34$; — —, $r = 0{\cdot}96$, $m = 0{\cdot}25$; — – —, $r = 0{\cdot}95$, $m = 0{\cdot}20$.

When the resonance frequencies are the same, the model overlap becomes infinite. This only occurs for the special case of two coupled oscillators.

The results presented in Figures 6 and 7 confirm that, in case of weak coupling, C_S can be highly sensitive to the uncoupled resonance frequencies ratio. However, there is seen to be a convergence of curves in Figures 6 and 7 as k is increased. The same calculations have been performed with resonance frequency ratios greater than unity or with $\eta_1 = 5 \times 10^{-3}$ and a similar convergence of curves is observed [3]. In each case, the convergence occurs for C_S between 0·05 and 0·07. This directly relates to the transition zone between weak and strong coupling coloured in grey in the figures. Before the convergence, the coupling is weak and the temporal evolution of the impulse response is sensitive to the values of the uncoupled resonance frequencies. After the convergence, the coupling is strong, C_S is small, the impulse response is dominated by global modes and therefore it is not sensitive to the values of uncoupled resonance frequencies. In this respect, the choice of 0·07 as a threshold for C_S seems relevant.

Whatever the ratio between the uncoupled resonance frequencies, when the coupling is strong these uncoupled resonance frequencies do not affect the dynamic behaviour of the system. There are no localized modes and, therefore, there cannot be modal interaction between localized modes. It is remarkable that the value of coupling stiffness, k, for which the coupling can be considered as strong does not depend on the uncoupled frequency ratio, r. So long as uncoupled resonance frequencies are sufficiently proximate to produce a value of C_S greater than 0·07 in case of *very weak coupling* (horizontal regions of the curves), C_S stays above 0·07 in the *whole region of weak coupling* defined for $r = 1$ (perfect modal coincidence and $C_S > 0{\cdot}07$). This is typically the case when $0{\cdot}992 \leqslant r \leqslant 1$ in Figure 6 and when $0{\cdot}96 \leqslant r \leqslant 1$ in Figure 7. This behaviour is very significant and has been confirmed for more complex systems such as two coupled plates [3]. Therefore, if a criterion related to modal interaction ensures that C_S is greater than 0·07 in the case of very weak coupling, then this criterion will also ensure that C_S is greater than 0·07 so long as the coupling is not strong. This conclusion is very important insofar as it enables the use of the mathematical model of two oscillators in case of *very weak coupling* to design a criterion which could be generalized to the whole region of weak coupling without restriction.

4. THE CASE OF TWO VERY WEAKLY COUPLED MODES

4.1. DESCRIPTION OF THE MATHEMATICAL MODEL

In reference [6], it is demonstrated that in case of very weak coupling, i.e., when $k^2/\omega_1 d_1 \omega_2 d_2 \ll 1$, according to equation (3) displacement $\tilde{X}_2$ is approximately inversely proportional to the product of modal impedances,

$$\tilde{X}_2 = \frac{k}{(-m\omega^2 + K_1 + k + \mathrm{i}d\omega)} \frac{1}{(-m\omega^2 + K_2 + k + \mathrm{i}d\omega)}. \tag{6}$$

Then, the temporal evolution of the local kinetic energy of the indirectly excited oscillator may be analytically derived from equation (6):

$$E_2(t) = \frac{1}{\lambda^2} \times \frac{1}{m^2} \times \{\cos^2(\omega_2^d t - \Theta_{21})\, \mathrm{e}^{-\eta_2 \omega_2 t} + \cos^2(\omega_1^d t - \Theta_{12})\, \mathrm{e}^{-\eta_1 \omega_1 t} \cdots$$
$$- 2\cos(\omega_2^d t - \Theta_{21}) \cos(\omega_1^d t - \Theta_{12})\, \mathrm{e}^{-(\eta_1/2)\omega_1 t}\, \mathrm{e}^{-(\eta_2/2)\omega_2 t}\}, \tag{7}$$

where $\omega_1 = \sqrt{K_1/m}$ and $\omega_2 = \sqrt{K_2/m}$. λ, Θ_{21} and Θ_{12} do not depend on time and are defined in Appendix A.

It is suggested in reference [5] that this model is also valid to represent the behaviour of two very weakly coupled modes. Furthermore, in SEA, when coupling is weak, the interaction between modes of connected substructures is described on a mode-to-mode basis. The dynamics of each subsystems are represented by a set of oscillators and the characteristics of the energy flow are described while considering two coupled oscillators at a time [6]. Therefore, all numerical results relying upon this mathematical model of two very weakly coupled oscillators are likely to be valid for two very weakly coupled modes. Besides, although this model is valid only in case of *very* weak coupling, it has been suggested in the previous section that, as far as modal interaction is concerned, it is likely to yield conservative criteria to ensure modal interaction in any case of weak coupling.

According to equation (7), the temporal moving average of $E_2(t)$ yields C_S as a function of four variables,

$$C_S(\omega_1, \omega_2, \eta_1, \eta_2).$$

C_S as a function of four variables is carefully studied in the following sections. This consists in looking for the quadruplets $(\omega_1, \omega_2, \eta_1, \eta_2)$ for which $C_S = 0{\cdot}07$. An iterative method is used. All the variables are fixed except one. To establish the value of the remaining variable for which $C_S = 0{\cdot}07$, a bisection method [7] is used. It is particularly appropriate insofar as, beforehand, it has been checked that C_S as a function of one variable is globally monotonic. With a dichotomic procedure, the criterion of convergence is directly related to the precision desired to solve the equation. This is illustrated in the next section. Following all these numerical studies, a criterion to predict modal interaction between two modes will be proposed.

4.2. $C_S(\omega_1, \omega_2) = 0{\cdot}07$

In this section, η_1 and η_2 are fixed and the equation $C_S(\omega_1, \omega_2) = 0{\cdot}07$ is solved. This equation is solved with a convergence criterion of 3×10^{-3}. This means that if (ω_1, ω_2) is a solution, then $0{\cdot}067 < C_S < 0{\cdot}073$. This value for the precision has been chosen in order to accelerate the convergence of the algorithm used to solve the equation without substantially altering the results. The equation $C_S(\omega_1, \omega_2) = 0{\cdot}07$ defines a curve. However, rather than plotting this curve, the curve defined by $C_S(\omega_1, \omega_2/\omega_1) = 0{\cdot}07$ is presented in Figure 8. This result suggests that for given damping ratios, a sensible parameter related to modal interaction is not ω_1–ω_2 but rather ω_2/ω_1. The greater the ω_1, the less close ω_2 need to be to ω_1 to produce modal interaction. For a given damping ratio, the two modes need to be closer at lower frequency to ensure modal interaction. The two straight lines related to given damping ratios clearly define two zones. If the frequency ratio is between the two straight lines, then the modes are proximate enough to yield $C_S > 0{\cdot}07$ in case of weak coupling. There is modal interaction. But, if the frequency ratio is outside the two straight lines, then the two modes are too far apart, and C_S will remain less than 0·07 even if the modes are weakly coupled. In this latter case, C_S is of no use for detecting weak coupling.

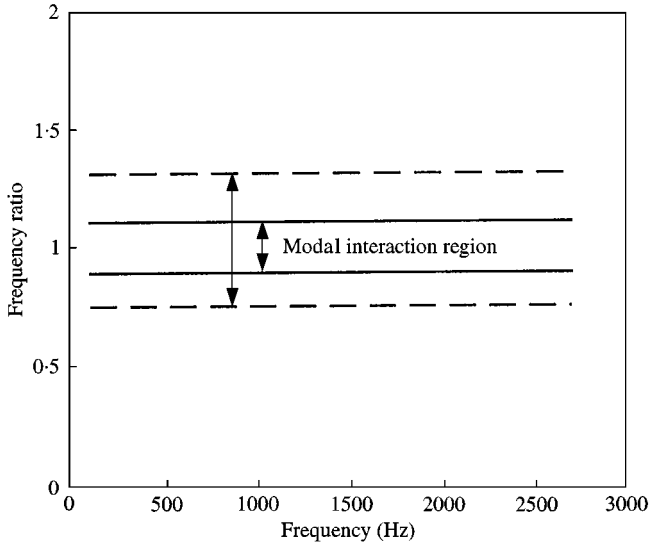

Figure 8. Frequency ratio for modal interaction as a function of frequency: ——, $\eta_1 = 10^{-2}$, $\eta_2 = 1{\cdot}2 \times 10^{-2}$, – –, $\eta_1 = 4 \times 10^{-2}$, $\eta_2 = 1{\cdot}2 \times 10^{-1}$.

Furthermore, although two zones have been very clearly defined, it is very important to know if the transition between them is sharp or not. This is directly related to the sensitivity of C_S to small variations of frequency ratio, and therefore to modal density. Three different cases have been considered. In each case, C_S as a function of $r = \omega_2/\omega_1$ has been derived with $\omega_1 = 2\pi \times 1000$ rad/s (Figure 9). Around $C_S = 0{\cdot}07$, C_S as a function of frequency ratio (r) has been approximated by a polynomial curve with the Polyfit function of MATLAB. The derivatives of the polynomial curves provide an evaluation of the sensitivity of C_S to small changes in r when C_S value is around 0·07. Indeed, the derivatives may be expressed as $\partial C_S/\partial r \cong \Delta C_S/\Delta r$, where Δr denotes a small change in the frequency ratio r and ΔC_S is the resulting change in C_S. Table 2 yields the estimated values for the derivatives in three cases.

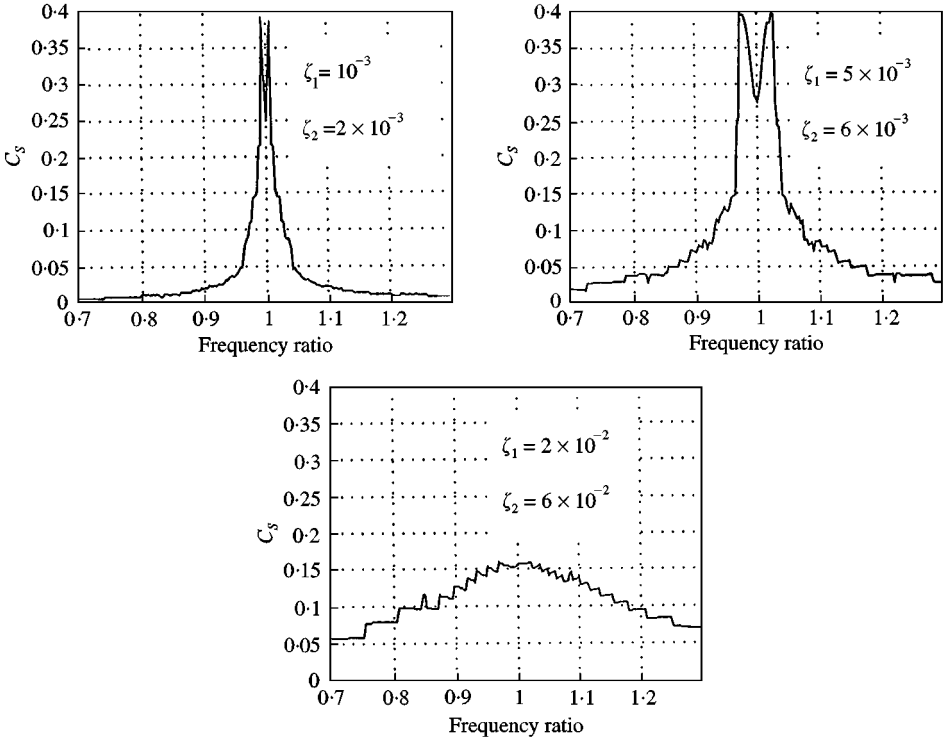

Figure 9. Sensitivity of C_S to frequency ratio.

TABLE 2

Sensitivity of C_S to frequency ratio

	$\eta_1 = 2 \times 10^{-3}$ $\eta_2 = 4 \times 10^{-3}$	$\eta_1 = 10^{-2}$ $\eta_2 = 1{\cdot}2 \times 10^{-2}$	$\eta_1 = 4 \times 10^{-2}$ $\eta_2 = 1{\cdot}2 \times 10^{-1}$
$\frac{\partial C_S}{\partial r}$ for $r < 1$	3.44	0.70	0.43
$\frac{\partial C_S}{\partial r}$ for $r > 1$	− 3·44	− 0·52	− 0·18

According to Table 2, when C_S is around 0·07, a change, Δr, equal to or less than 10^{-3} in the frequency ratio would yield a change ΔC_S less than or equal to $3{\cdot}44 \times \Delta r$ for the range of damping considered. However, for $\eta_1 = 10^{-2}$ and $\eta_2 = 1{\cdot}2 \times 10^{-2}$, ΔC_S would only decrease to $0{\cdot}70 \times \Delta r$. It is worth noting that the robustness of C_S to changes in the frequency ratio increases with damping. Typically, if for $r = r_0$, $C_S = 0{\cdot}07$, then for $r = r_0 \pm 0{\cdot}001$,

$$0{\cdot}07 - 3{\cdot}44 \times 10^{-3} < C_S < 0{\cdot}07 + 3{\cdot}44 \times 10^{-3}$$

or

$$0{\cdot}066 < C_S < 0{\cdot}074.$$

This means that if the frequency ratio yielding $C_S = 0{\cdot}07$ is known with a precision equal to 10^{-3}, then the previous equality is true with an error less than 0·004. It is therefore unnecessary to require a greater precision for r. Thus, in Figure 8, for practical damping values, the transition zone defined by the straight lines is quite robust against small changes in frequency ratio. As we will see in section 5, this implies that C_S is also robust against small changes in modal density. The following derivations are based upon this conclusion.

Once the damping is fixed, the range of ω_2/ω_1 in which C_S is equal to 0·07 can be derived. This allows us to evaluate the reliability of the indication given by C_S. If the actual frequency ratio is between the two transition values, then a reliable assessment of strength of coupling can be performed with C_S; otherwise C_S is of no use insofar as it can be less than 0·07 even if the two modes are weakly coupled. It can also be noticed in Figure 8 that the transition values for the frequency ratios are highly dependent on damping ratios. Therefore, in the next section, the influence of damping on modal interaction is studied.

4.3. $C_S(\eta_2, \omega_2/\omega_1) = 0{\cdot}07$

For a given pair (ω_1, η_1) and a value η_2, the values of ω_2/ω_1 for which $C_S = 0{\cdot}07 \pm 0{\cdot}03$ have been derived (Figure 10).

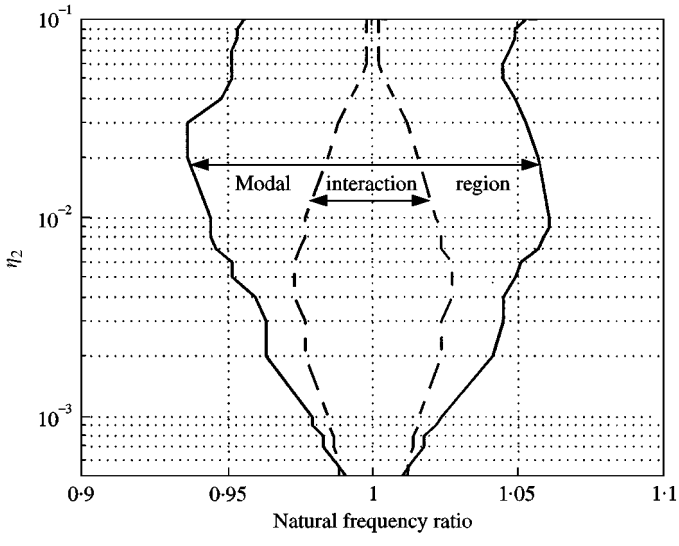

Figure 10. Influence of natural frequency ratio and loss factors on modal interaction: ——, $\eta_1 = 5{\cdot}1 \times 10^{-3}$; — – —, $\eta_1 = 1{\cdot}1 \times 10^{-3}$.

Modal interaction seems to be related to modal bandwidth when both values of damping have the same order of magnitude. In this case, the wider is one of the modal bandwidths, the wider is the region of modal interaction between the models. However, the combined influence of loss factors has not yet been studied. Section 4.2. has shown that C_S is not a function of $(\omega_1, \omega_2, \eta_1, \eta_2)$ but rather a function of $(\omega_2/\omega_1, \eta_1, \eta_2)$. As a function of three variables, the solution of the equation $C_S(\eta_1, \eta_2, \omega_2/\omega_1) = 0{\cdot}07$ can be represented by a surface. This has been done in the next section.

4.4. $C_S(\omega_2/\omega_1, \eta_1, \eta_2) = 0{\cdot}07$

The equation $C_S(\omega_2/\omega_1, \eta_1, \eta_2) = 0{\cdot}07$ has been solved for $(\eta_1, \eta_2) \in [10^{-3}; 10^{-1}] \times [10^{-3}; 10^{-1}]$. For 19×19 pairs (η_1, η_2), the two values of ω_2/ω_1 for which $C_S = 0{\cdot}07 \pm 0{\cdot}01$ have been derived. A precision of 0·1 has been chosen to reduce the computing time. Despite this low precision, the convergence has not always been established. Sometimes, the position of the maximum of moving average of the energy impulse response seems to be extremely sensitive to small changes in frequency ratio. This happens when the moving average has two peaks whose magnitudes are very close. A very small change in the natural frequency ratio makes the maximum "jump" from one peak to the other making C_S "jump" from one value to the other. If $0{\cdot}07 \pm 0{\cdot}01$ is between these two values, the algorithm cannot converge. Rather than ignoring the pairs of loss factors for which this phenomenon occurs, it has been arbitrarily decided to stop the algorithm when the change in frequency ratio from one iteration to the other is less than 0·001 and to retain as a result the value of the frequency ratio attained. This is subsequently justified. Figure 11 and 12 illustrate the results. When both modal bandwidths are large, modal interaction seems easily ensured.

All the numerical results for the 19×19 pairs (η_1, η_2) are presented in Appendix B. The pairs for which the algorithm has not converged are indicated by a dark-grey background. It is worth noting that the questioned values are totally coherent with the rest of the table therefore justifying the approximation. Moreover, insofar as, for a given system, the values for the frequencies are supposed to be fixed, this phenomenon of instability does not really alter the deterministic measure of C_S. However, from a statistical point of view, it deserves more attention because it can greatly modify the confidence interval related to C_S and modal interaction.

As a result of these numerical studies, the phenomenon of modal interaction is better understood, or at least quantified. For given loss factors, the higher are the frequencies, the less close they need to be to ensure modal interaction (Figures 11 and 12). For reasonable damping, the greater the loss factors, the less proximate natural frequencies need to be. It thus appears that, in case of two coupled modes, modal interaction depends on modal bandwidth. These results are the basis for the proposal of a modal interaction indicator for multi-modal systems in the next section.

5. MODAL INTERACTION: THE CASE OF MULTI-MODAL COUPLING

5.1. M_p: A CRITERION FOR MODAL INTERACTION

In the previous section, a conservative condition has been derived to ensure modal interaction. If this condition is fulfilled and C_S is less than 0·07, this means that there is strong coupling. This condition has been derived for two coupled modes and involves both natural frequencies and damping ratios. In practice, within a frequency band, every particular resonance frequency and damping ratio related to the uncoupled subsystems are

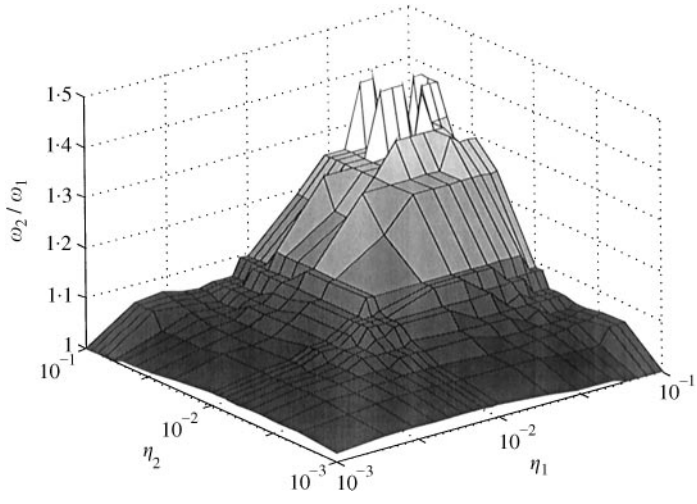

Figure 11. Modal interaction surface as a function of loss factors and natural frequency ratio. Case of natural frequency ratio greater than 1.

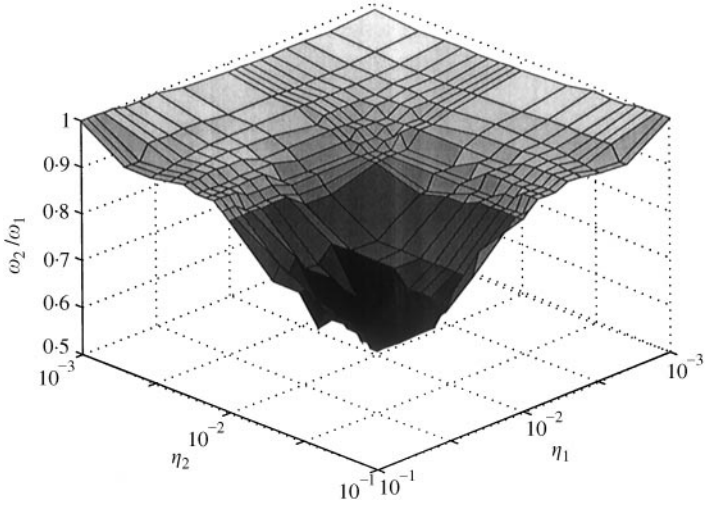

Figure 12. Modal interaction surface as a function of loss factors and natural frequency ratio. Case of natural frequency ratio less than 1.

impossible to measure. This is especially true when the modal overlap is high. However, in most practical cases, modal density of both subsystems, n_1 and n_2, and their internal loss factors, η_1 and η_2, can be estimated reasonably reliably. This section aims at adapting the previous condition to practical cases for which modal densities and internal loss factors are the only available data. In section 4.2, for given loss factors (η_1, η_2), it has been shown that existence of modal interaction does not depend on distance between two uncoupled natural frequencies ω_1 and ω_2 but rather on their ratio ω_2/ω_1. Let us denote by $x_{min} = \omega_2/\omega_1|_{min}$ and $x_{max} = \omega_2/\omega_1|_{max}$ the two natural frequency ratios between which modal interaction exists (Figure 8). The indication provided by C_S is related to the strength of coupling as long

as there exist two natural frequencies ω_1 and ω_2 such that

$$x_{min} < \frac{\omega_2}{\omega_1} < x_{max}. \tag{8}$$

For practical SEA analysis, coupling loss factors and internal loss factors are always derived over a frequency band. Therefore, it is highly desirable to extend the condition (8), valid only for two coupled modes, to a whole frequency band. So, it is assumed that ω_1 and ω_2 are within the frequency band $[\omega_{min}; \omega_{max}]$.

Since

$$|\omega_1 - \omega_2| < \omega_{min} \min(|1 - x_{min}|, |1 - x_{max}|) \Rightarrow \left|1 - \frac{\omega_2}{\omega_1}\right| < \min(|1 - x_{min}|, |1 - x_{max}|)$$

$$\left|1 - \frac{\omega_2}{\omega_1}\right| < \min(|1 - x_{min}|, |1 - x_{max}|) \Rightarrow x_{min} < \frac{\omega_2}{\omega_1} < x_{max}, \tag{9}$$

the new condition for modal interaction within a frequency band might than be written as

$$|\omega_1 - \omega_2| < \omega_{min} \min(|1 - x_{min}|, |1 - x_{max}|). \tag{10}$$

Condition (10) is conservative according to equation (9), condition (10) implies condition (8). x_{min} and x_{max} depend on the internal loss factors and ω_{min} is related to the frequency band considered. Equation (10) is valid as long as x_{min} and x_{max} remain approximately constant over the frequency band. This means that damping must be also almost uniform over the frequency band considered.

Condition (10) relates modal interaction to the distance between uncoupled modes; therefore it is important to assess the separations between each set of uncoupled modes. If very weak coupling is assumed for the whole frequency band considered, according to reference [3], modal interaction occurs when only two uncoupled modes are sufficiently proximate.[†] Therefore, the parameter directly related to modal interaction is the *smallest* of all the separations between the uncoupled modes. Let us denote by $dist_{min}$ this parameter. In case of modal coincidence, $dist_{min} = 0$. But, usually, it is greater than zero. There is modal interaction if $dist_{min} < \omega_{min} \min(|1 - x_{min}|, |1 - x_{max}|)$. So, a modal interaction indicator can be defined by

$$M_p = \frac{\omega_{min} \min(|1 - x_{min}|, |1 - x_{max}|)}{dist_{min}}, \tag{11}$$

where x_{min} and x_{max} are derived for *given internal loss factors.*

If M_p is greater than unity, there is model interaction and C_S is a good indicator of strength of coupling; but if M_p is less than unity and C_S is less than 0·07, then there is no definite conclusion about the strength of coupling. The major difficulty in deriving M_p is the assessment of $dist_{min}$. Unless the two subsystems are very well defined, a deterministic approach does not seem appropriate. Besides, SEA usually deals with practical structures subject to uncertainties. Therefore, a statistical assessment of $dist_{min}$ appears to be the most pertinent from a practical point of view.

[†] We write "two uncoupled modes" but in fact, this means one uncoupled mode from the first subsystem and the other from the second subsystem.

5.2. A STATISTICAL APPROACH TO ASSESSING $dist_{min}$

In order to assess the statistics of $dist_{min}$, the statistical distributions of the uncoupled natural frequencies of both subsystems are required. In the absence of any definite conclusion, the same statistical distribution as that used by Lyon [6] to derive the main parameters of SEA has been chosen. The mode distribution within the frequency band *is assumed to be uniform* for both very weakly coupled subsystems. The uncoupled natural frequencies are assumed to be independent stochastic variables. On average, for a system with two sets of uncoupled modes drawn with a uniform probability, $dist_{min}$ is greater than zero. Insofar as the probability distribution of the uncoupled modes is known, it is possible to derive the probability distribution of $dist_{min}$. The chosen method is a Monte Carlo simulation. Two vectors of size respectively N_1 and N_2 represent the two sets of uncoupled natural frequencies. Their components are drawn with a uniform probability between 0 and 1. N_1 is the number of modes within the chosen frequency band for the first subsystem whereas N_2 is related to the other subsystem. N_1 and N_2 are the only two parameters. There are directly related to modal density. Once the two vectors have been drawn, $dist_{min}$, the smallest frequency separation between these two sets of uncoupled natural frequencies is derived. If the frequency band is $[\omega_{min}; \omega_{max}]$ instead of [0; 1], we just multiply $dist_{min}$ by $\omega_{max} - \omega_{min}$. The procedure is repeated 20 000 times to yield an estimate of the average and standard deviation of $dist_{min}$ which is not sensitive to the number of draws. Besides, with 20 000 values for $dist_{min}$, it becomes possible to assess quite precisely its cumulative probability distribution. Let us denote by μ the average of $dist_{min}$ and by σ its standard deviation. μ and σ have been derived for N_1 and N_2 varying between 1 and 20. This yields 20×20 values for the average and standard deviation of $dist_{min}$. It is suggested in reference [3], that both average, μ, and standard deviation, σ, can be approximated by the same analytical formula,

$$\mu(N_1, N_2) = \frac{1}{2}\frac{1}{N_1 N_2},$$

$$\sigma(N_1, N_2) = \frac{1}{2}\frac{1}{N_1 N_2}. \tag{12}$$

Furthermore, the probability distribution of $dist_{min}$ appears to be related to a particular Gamma distribution (Figure 13) defined by

$$f(x) = \begin{cases} \dfrac{1}{\mu} e^{-\frac{x}{\mu}} & x > 0,\ \mu > 0, \\ 0 & \text{otherwise}, \end{cases}$$

and its cumulative probability distribution is defined by $F(x) = \int_{u=0}^{x} (1/\mu)\, e^{-u/\mu}\, du$.

Although this has been checked for most of the simulated cases, it would be worth demonstrating it analytically for arbitrary values of N_1 and N_2.

On the basis of the analytical approximations, the probability distribution for $dist_{min}$ can be predicted whatever the number of uncoupled modes. Let us denote by $\Delta\Omega_{90}$, the limit below which are 90% of $dist_{min}$ values. This limit can be found on the basis of the cumulative distribution function of the associated gamma distribution (Figure 13). It is defined by

$$F(\Delta\Omega_{90}) = 0{\cdot}9,$$

hence

$$\Delta\Omega_{90} = -\mu \ln(1 - 0{\cdot}9). \tag{13}$$

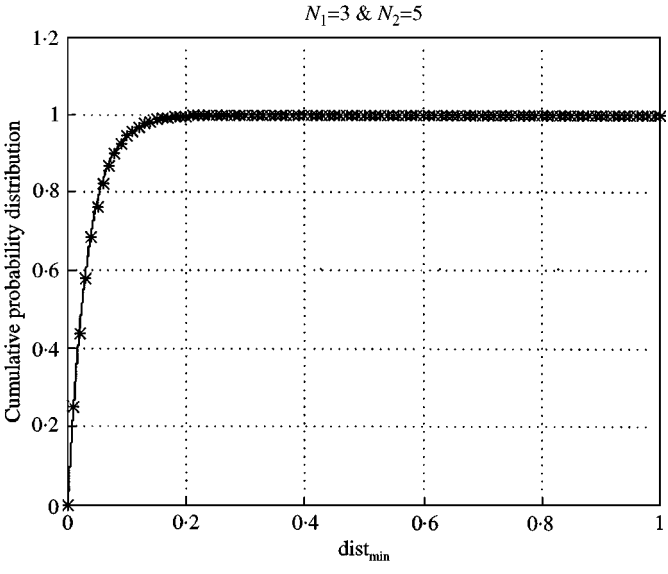

Figure 13. Cumulative probability distribution of $dist_{\min}$ in case of a uniform probability distribution of the uncoupled natural frequencies for $N_1 = 3$ and $N_2 = 5$. $*$ Gamma distribution; ——Numerical simulation

$\Delta\Omega_{90}$ depends not only on N_1 and N_2 but also on the frequency bandwidth. If $\Delta\Omega_{90}$ is less than the required separation between two natural frequencies to have modal interaction, this means that for 90% of the coupled sets of modes drawn from a uniform population there exist at least two modes proximate enough to ensure modal interaction. For the particular probability distribution used for the uncoupled natural frequencies, the modal interaction indicator might be written as

$$M_p = \frac{\omega_{min}\ \min(|1 - x_{min}|, |1 - x_{max}|)}{\Delta\Omega_{90}}, \tag{14}$$

where x_{min} and x_{max} are derived for *given internal loss factors.*

M_p has been defined for a given frequency band and internal loss factors are assumed to be constant over the frequency band. In the following section, some application of M_p to various systems are presented. The results are compared with previous studies.

5.3. APPLICATION OF M_p TO VARIOUS SYSTEMS

In this section, M_p is applied to the five systems studied in references [1, 2]. Rather than using the Gamma distribution values for $\Delta\Omega_{90}$, some numerical simulations have been performed to derive its exact value. The only difference observed with the approximated values is for $N1 = N2 = 1$. For all the other cases, the relative error is less than 2%. In practice, the experimenter assesses the number of modes N_1 and N_2 in the frequency band. Then, it is very easy to derive $\Delta\Omega_{90}$ using equations (12) and (13). Furthermore, if the internal loss factors have been measured, then the appropriate values for x_{min} and x_{max} may be found in Appendix B. Therefore, it becomes possible to derive M_p. The only data required beforehand are the modal densities and internal loss factors for each subsystems.

5.3.1. *Two coupled rods: numerical simulations*

For a uniform, isotropic, one-dimensional system, the modal density is $n = L/\pi\, c_g$ where L is the length of the system and c_g the group velocity. For a rod, $c_g = \sqrt{E/\rho}$ with E, the Young's modulus and ρ the density and the modal density is actually uniform. In reference [1], the effect of proximate modes on C_S has been carefully studied for two clamped-free rods coupled by a spring and subject to quasi-longitudinal waves. Therefore, it has been decided to consider the same rods. In reference [1], the two coupled rods have the same internal loss factors. Whereas $n(\omega)$ does not depend on the circular frequency ω, damping is inversely proportional to ω. It varies so much within the frequency band considered in reference [1] that it has been decided to examine different parts of the frequency band containing at least one natural frequency. For each frequency band the minimum and maximum values of internal loss factors have been derived. The values used to derive M_p are presented in Table 3.

For each frequency band and each values of internal loss factors, x_{min} and x_{max} have been obtained from Appendix B and M_p has been assessed. The results are listed in Table 4. A synthesis of all the possible values for M_p in each frequency band is presented in the last column of Table 4. Of course, in practice, there should be only one value of internal loss factor per frequency band and a single value for M_p.

Whichever the frequency band considered, M_p is less than unity. Thus, according to the new criterion, Table 4 indicates that, on a statistical basis, there is modal interaction. Therefore, the ability of C_S to distinguish weakly from strongly coupled subsystems in a SEA sense is highly sensitive to separation between uncoupled resonance frequencies. The conclusion raised by the new criterion totally agrees with the results presented in reference [1]. When the length of the coupled rods is varied, the value of C_S may be less than 0·07, therefore misleading the experimenter who would believe that the rods are strongly coupled. However, two coupled rods is the most simple system and the new criterion has been tested on more complex structures.

TABLE 3

Input data used to derive M_p in the case of two coupled rods

Frequency band (rad/s)	[500; 1000]	[1000; 3000]	[3000; 6625]
Internal loss factors	$\eta_{min} = 4{\cdot}8 \times 10^{-3}$ $\eta_{max} = 9{\cdot}7 \times 10^{-3}$	$\eta_{min} = 1{\cdot}6 \times 10^{-3}$ $\eta_{max} = 4{\cdot}8 \times 10^{-3}$	$\eta_{min} = 8 \times 10^{-4}$ $\eta_{max} = 1{\cdot}6 \times 10^{-3}$
Number of modes	$N_1 = N_2 = 1$	$N_1 = N_2 = 2$	$N_1 = N_2 = 3$

TABLE 4

Results obtained for M_p in the case of two coupled rods

	$\lvert 1 - x_{min} \rvert$		$\lvert 1 - x_{max} \rvert$		$\Delta\Omega_{90}$	$\omega \min(\lvert 1 - x_{min} \rvert, \lvert 1 - x_{max} \rvert)$		M_p
	min	max	min	max		min	max	
[500; 1000]	0·06	0·12	0·06	0·12	342·5	30	120	$< 0{\cdot}35$
[1000; 3000]	0·02	0·06	0·02	0·06	570.0	20	180	$< 0{\cdot}31$
[3000; 6625]	0·01	0·02	0·01	0·02	478·4	30	132·5	$< 0{\cdot}28$

5.3.2. *Two coupled beams: numerical simulations*

The two beams considered are the same as those studied in reference [1]. The systems consist of ideal Euler–Bernoulli cantilever beams in flexure coupled by a spring. The beams are uniform, homogenous one-dimensional systems, so their modal density might be expressed as $n = L/\pi c_g$ where L is the length of the system and c_g is the group velocity. Unlike the compressive waves, the bending waves are dispersive, so the group speed depends on frequency; it is twice the phase speed. The mode distribution is not uniform. For the two beams considered in reference [1], the internal loss factors are the same. The main values necessary to derive the criterion are presented in Table 5.

For each frequency band, x_{min} and x_{max} have been obtained from Appendix B and M_p has been assessed. The results are listed in Table 6. A synthesis of all the possible values for M_p is presented in the last column of Table 6 for each frequency band.

Table 6 shows that, on a statistical basis, modal interaction is not ensured for the two coupled beams. Once more, this conclusion agrees with the results presented in reference [1]. C_S might be less than 0·07 even if the subsystems are weakly coupled.

5.3.3. *Two rectangular coupled plates: numerical simulations*

In this section, the system consists of two rectangular mild steel plates of equal width. The two plates are homogeneous, isotropic and very thin as compared to the wavelength involved. Each plate has two opposite sides simply supported. The plates are coupled together along one edge with a uniform line coupling element which allows translational as well as rotational motions of the coupled edges. The coupling element is conservative and the remaining edges of the two plates (opposite to the coupling line) are clamped. The system is subjected to flexure. The physical characteristics of both plates are similar to those presented in reference [1]. The frequency band considered in reference [1] is [50; 134] rad/s. The actual number of modes within the frequency bands is $N_1 = N_2 = 8$ and the damping varies from $3{\cdot}8 \times 10^{-3}$ to 10^{-2}. The results obtained for M_p are presented in Table 7.

TABLE 5

Input data used to derive M_p in the case of two coupled beams

Frequency band (rad/s)	[37; 700]	[700; 2500]	[2500; 3500]
Internal loss factors	$\eta_{min} = 7{\cdot}4 \times 10^{-3}$ $\eta_{max} = 9 \times 10^{-2}$	$\eta_{min} = 2 \times 10^{-3}$ $\eta_{max} = 7{\cdot}4 \times 10^{-3}$	$\eta_{min} = 1{\cdot}5 \times 10^{-3}$ $\eta_{max} = 2 \times 10^{-3}$
Number of modes	$N_1 = N_2 = 1$	$N_1 = N_2 = 2$	$N_1 = N_2 = 1$

TABLE 6

Results obtained for M_p in the case of two coupled beams

	$\lvert 1 - x_{min} \rvert$		$\lvert 1 - x_{max} \rvert$		$\Delta\Omega_{90}$	$\omega \min(\lvert 1 - x_{min} \rvert, \lvert 1 - x_{max} \rvert)$		M_p
	min	max	min	max		min	max	
[37; 700]	0·10	0·25	0·10	0·25	188·9	3·7	175	$< 0{\cdot}92$
[700; 2500]	0·03	0·10	0·03	0·10	513.0	21	250	$< 0{\cdot}49$
[2500; 3500]	0·03	0·03	0·03	0·03	685·0	75	105	$< 0{\cdot}16$

TABLE 7

Results obtained for M_p in the case of two coupled plates

	$\lvert 1 - x_{min} \rvert$		$\lvert 1 - x_{max} \rvert$		$\Delta\Omega_{90}$	$\omega \min(\lvert 1 - x_{min} \rvert, \lvert 1 - x_{max} \rvert)$		M_p
	min	max	min	max		min	max	
[50; 134]	0·04	0·10	0·04	0·10	1·51	2	13·40	$> 1{\cdot}32$

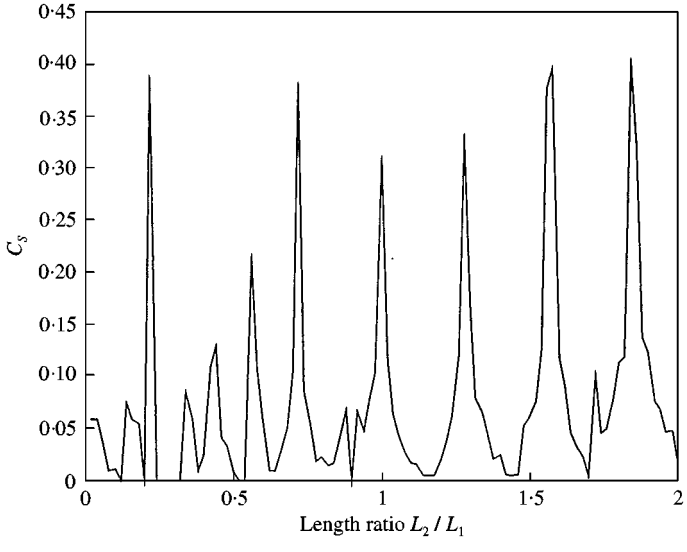

Figure 14. $K_t = 10$ N/m^2 and $K_t = 10$ N/rad.

According to Table 7, M_p is greater than unity. This means that, on a statistical basis, there is modal interaction: C_S should not be sensitive to changes in natural frequencies location. However, the results presented in reference [1] contradict this conclusion. In Figure 14, C_S appears to be highly sensitive to the length ratio of the two coupled plates. L_1 and L_2 are respectively the length of the plates measured along the simply supported edges. For $L_2/L_1 = 0{\cdot}9$, $C_S = 0{\cdot}01$. To confirm this result, C_S has been derived for 25 randomly chosen points — five excitation points chosen on one plate and five points, where the dynamic response is measured, chosen on the other plate. Therefore, 25 values of C_S have been derived. The 90% confidence interval is [0·0791; 0·1883]. This clearly shows that there is modal interaction.

It becomes obvious that the spatial distribution of modes is very important. In this particular case, M_p is quite small. This means that in the neighbourhood of each uncoupled mode of the first plate there is only one or two uncoupled modes of the second plate. Moreover, there is a time delay only if the mode shapes of these close uncoupled modes match at the boundary. There is only a small number of uncoupled modes which fulfil the two conditions to yield a time delay. This is why, sometimes it might be difficult to excite two close uncoupled modes whose mode shapes are compatible at the coupling and this generates a statistical dispersion over the values of C_S (Figure 15).

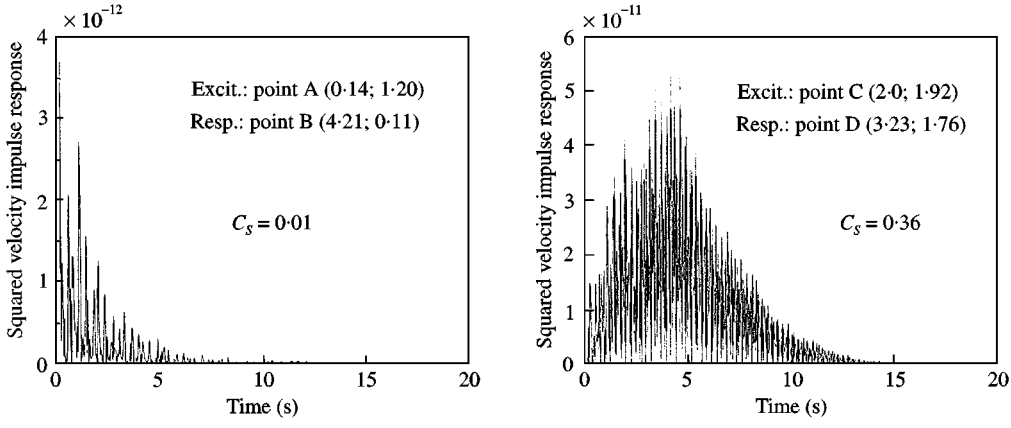

Figure 15. $K_t = 10$ N/m^2 and $K_t = 10$ N/rad. $L_{rat} = 0{\cdot}9$. Examples of squared velocity impulse response measured at two locations for two different excitation points (the co-ordinates of the points are related to the reference system used [1]).

C_S appears to be extremely sensitive to location of excitation and response. This dispersion of measures arises from low modal density combined with a 2D system. To measure a significant C_S, there have to be resonance frequencies *and* mode shapes matching. M_p does not take into account this latter requirement. Depending on the location of excitation and response, the two proximate modes may not be excited or observed. Nevertheless, it should be remembered that this analysis has been based on geometrically regular systems in which selectivity is extreme. Finite element studies by Mace [8] of the effect of irregularity on energy distribution between subsystems show that significant cross-modal interaction occurs at higher levels of damping for rectangular regular systems.

From a practical point of view, whenever it is possible, it is worth performing several measures of C_S and deriving confidence limits. The use of confidence intervals derived from a sample of values for C_S helps the experimenter to be confident in the results.

5.3.4. *Two coupled plates*: *experiments*

The system consists of two coupled 3 mm thick steel plates of irregular shape and identical material properties (Figure 16). The two plates are coupled by means of 3 mm thick steel straps of 40 and 50 mm free length. The two plates considered in this section are the same as those presented in reference [2]. Their dimensions and the experimental set-up may be found in references [2]. The measurements of damping and modal densities for both plates may be found in reference [9]. Some internal loss factors values have been extrapolated. The experimental data used to derive M_p are listed in Table 8.

All the frequency bandwidths equal to 200 Hz. Thus, $\Delta\Omega_{90}$ is the same whatever the frequency band. In all cases, $N_1 = n_1 \times 200 \cong 13$ and $N_2 = n_2 \times 200 \cong 18$. ($x_{min}$, x_{max}) has been obtained from Appendix B. The values for M_p are listed in Table 9.

According to Table 9, whatever are frequency band, there is always modal interaction. The conclusion is not contradicted by the experimental results presented in reference [2] for which confidence intervals were derived.

5.3.5. *Two rooms coupled by an aperture*: *experiments*

The two rooms considered are those presented in reference [2] (Figure 17). For these particular coupled systems, the damping could easily be varied by adding or removing

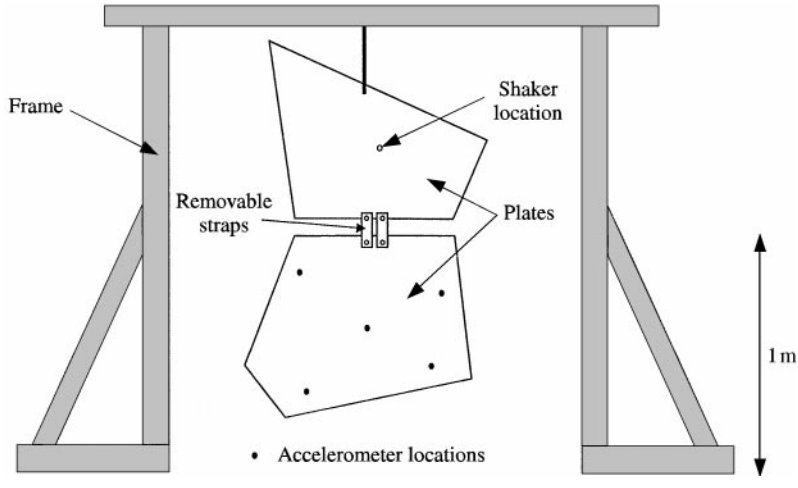

Figure 16. Two coupled plates.

TABLE 8

Internal loss factors and modal densities measured on two plates coupled by two straps [2]

Centre frequency (Hz)	Plate 1 $n_1(f)$	Plate 2 $n_2(f)$	Plate 1 η_1	Plate 2 η_2
200	0·0656	0·0926	$2{\cdot}74 \times 10^{-3}$	7×10^{-4}
600	0·0656	0·0926	$1{\cdot}92 \times 10^{-3}$	10^{-3}
1900	0·0656	0·0926	$1{\cdot}51 \times 10^{-3}$	8×10^{-4}
4900	0·0656	0·0926	7×10^{-3}	3×10^{-3}
6900	0·0656	0·0926	8×10^{-3}	4×10^{-3}

TABLE 9

Results obtained for M_p in the case of two coupled plates studied experimentally

	$\lvert 1 - x_{min} \rvert$	$\lvert 1 - x_{max} \rvert$	$\Delta\Omega_{90}$	$f_{min} \min(\lvert 1 - x_{min} \rvert, \lvert 1 - x_{max} \rvert)$	M_p
[100, 300]	0·02	0·02	0·98	2	2·04
[500, 700]	0·02	0·02	0·98	10	10·2
[1800, 2000]	0·01	0·01	0·98	18	18·4
[4800, 5000]	0·04	0·04	0·98	192	196
[6800, 7000]	0·04	0·04	0·98	272	278

absorbing panels. Three configurations of coupled rooms have been studied — no absorbing panel, five absorbing panels, 10 absorbing panels put in room 2. The modal density is highly dependent on frequency. In all cases, the smallest modal density within the frequency band has been used. Indeed, if M_p is greater than unity, then it would be also greater than unity for greater modal density. For each frequency band, modal densities and

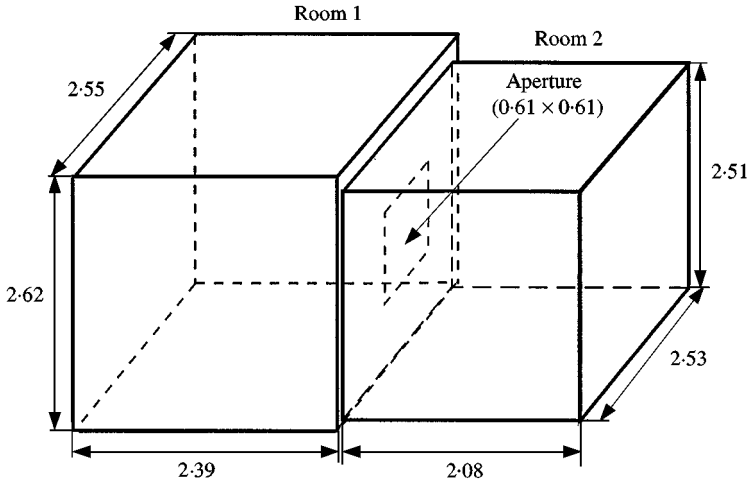

Figure 17. Two rooms coupled by an aperture; dimensions in m.

TABLE 10

Results obtained for M_p in the case of two coupled rooms studied experimentally

	No absorbing panel				
	$\lvert 1 - x_{min} \rvert$	$\lvert 1 - x_{max} \rvert$	$\Delta\Omega_{90}$	$f_{min} \min(\lvert 1 - x_{min} \rvert, \lvert 1 - x_{max} \rvert)$	M_p
[100, 500]	0·06	0·06	1·35	6	$> 4{\cdot}4$
[600, 1000]	0·03	0·03	$1{\cdot}032 \times 10^{-3}$	18	$> 17 \times 10^3$
[1600, 2000]	0·01	0·01	$2{\cdot}038 \times 10^{-3}$	16	$> 78 \times 10^4$

internal loss factors might be found in reference [2]. The value of M_p has been assessed for the three configurations of coupled rooms studied. The results for the configuration of coupled rooms with no absorbing panel is presented in Table 10.

It clearly appears that in all cases, there is modal interaction. The same conclusions have been reached for the two other configurations of coupled rooms [3]. This conclusion is very difficult to compare with any experimental results insofar as additional damping only "reinforces" modal interaction. However, the modal densities of both rooms are so high that it is not surprising that M_p indicates modal interaction.

6. CONCLUSION

The main drawback of C_S underlined in reference [1] is its sensitivity to modal proximity. C_S is only a reliable indicator when the modes localized within each subsystem interact. In this paper, an indictor of modal interaction M_p is proposed. It requires the assessment of modal densities and internal loss factors of the subsystems, a very simple numerical simulation and the use of Appendix B. If M_p is greater than unity then the indication provided by C_S is reliable and C_S is a good indicator of strength of coupling in a SEA sense. But, if M_p is less than unity and C_S is less than 0·07, then there is no possibility to distinguish

between strongly and weakly coupled subsystems. In all cases, when C_S is greater than 0·07, the coupling is weak. M_p and C_S appear to be complementary. M_p has been tested on the various experimental systems previously used to study C_S. The results are encouraging, but the lack of data and specifically designed tests precludes any definite conclusion about the validity of M_p. However, the indication provided by M_p could be of real importance. As long as C_S is greater than 0·07, the band-pass-filtered impulse response of the whole system is dominated by local modes. Therefore, from a SEA point of view, the structure can be divided into SEA subsystems. According to Langley [3], the SEA postulate is valid for this deterministic system. But, if M_p is less than unity, this means that a small change in the uncoupled natural frequencies location might alter in a spectacular way the band-pass-filtered response of the system. C_S could become less than 0·07 and it has been shown in reference [1] that, in this case, the magnitude of the response decreases by a large amount. Therefore, what is valid for a single system may not be valid for an ensemble of similar systems. M_p might be a good indicator of the equivalence between frequency-averaged data measured on a single structure and ensemble-average data.

However, the sensitivity analysis performed on C_S has revealed its limits for systems with very small dampling. Although the existence of the time delay to the peak of band-pass-filtered kinetic energy of the indirectly excited subsystem is not questioned, it would be worthwhile to test other procedure to be able to derive C_S for these extreme cases. For example, the uniform average used to derive the moving average could be replaced by an exponential average or a more appropriate averaging procedure. Another promising approach would be the use of the non-dimensional rise time proposed by Finnveden in reference [10]. In all cases, the same logic could be applied to design a modal interaction indicator.

Besides further investigations could be devoted to study the influence of the mode shapes matching on modal interaction

ACKNOWLEDGMENTS

The authors express their gratitude to Dr S. Finnveden for many helpful comments and discussions.

REFERENCES

1. F. J. FAHY and P. P. JAMES 1996 *Journal of Sound and Vibration* **190**, 363–386. A study of the kinetic energy impulse response as an indicator of the strength of coupling between SEA subsystems.
2. P. P. JAMES and F. J. FAHY 1997 *Journal of Sound and Vibration* **203**, 265–282. A technique for the assessment of strength of coupling between SEA subsystems: experiments with two coupled plates and two coupled rooms.
3. P. P. JAMES 1997 *Ph.D. Thesis*, *University of Southampton*. A Technique for the assessment of strength of coupling between statistical energy analysis subsystems.
4. R. S. LANGLEY 1989 *Journal of Sound and Vibration* **135**, 499–508. A general derivation of the statistical energy analysis equations for coupled dynamic systems.
5. P. P. JAMES and F. J. FAHY 1995 *ISVR Technical Report No*. 243. Evolution of the energy impulse response in the case of two very weakly coupled systems: a mathematical model.
6. R. H. LYON and R. DEJONG 1975 *Theory and Application of Statistical Energy Analysis*, second edition. Newton, MA Butterworth-Heinemann.
7. S. A. TEUKOSKY, B. P. FLANNERY, W. H. PRESS and W. T. VETTERING 1989 *Numerical Recipes in Fortran. The Art of Scientific Computing*, second edition. Cambridge University Press, Cambridge, UK.

8. B. R. MACE and P. J. SHORTER 1997 *Proceedings of the IUTAM Symposium on Statistical Energy Analysis*. Dordrecht: Kluwer Academic Publishers. Irregularity, damping and coupling strength in S.E.A.
9. F. J. FAHY and H. M. RUIVO 1997 *Journal of Sound and Vibration* **203**, 763–779. Determination of statistical energy analysis loss factors by means of an input power modulation technique.
10. S. FINNVEDEN 1997 *ISVR Technical Report No.* 268. Coupling strength as an indicator of the applicability of statistical energy analysis.

APPENDIX A

According to reference [4], λ, Θ_{21} and Θ_{12} are defined by

$$\lambda_2 = [(\zeta_1\omega_1 - \zeta_1\omega_2)^2 + (\omega_1^d)^2 - (\omega_2^d)^2]^2 + 4(\zeta_1\omega_1 - \zeta_2\omega_2)^2(\omega_2^d)^2,$$

$$\Theta_{12} = \Psi_{12} - \Lambda_1,$$

$$\Theta_{21} = \Psi_{21} - \Lambda_2,$$

where

$$\begin{cases} \cos(\Lambda_1) = \sqrt{1-\zeta_1^2}, \\ \sin(\Lambda_1) = \zeta_1, \end{cases} \quad \text{and} \quad \begin{cases} \cos(\Lambda_2) = \sqrt{1-\zeta_2^2}, \\ \sin(\Lambda_2) = \zeta_2, \end{cases}$$

and

$$\Psi_{12} = \arctan\left[\frac{-2(\zeta_1\omega_1 - \zeta_2\omega_2)\omega_1^d}{(\zeta_1\omega_1 - \zeta_2\omega_2)^2 - (\omega_1^d)^2 + (\omega_2^d)^2}\right],$$

$$\Psi_{21} = \arctan\left[\frac{2(\zeta_1\omega_1 - \zeta_2\omega_2)\omega_2^d}{(\zeta_1\omega_1 - \zeta_2\omega_2)^2 - (\omega_1^d)^2 + (\omega_2^d)^2}\right].$$

APPENDIX B

The numerical results for the 19×19 pairs (η_1, η_2) are presented in Tables 11 and 12. The two bold lines and columns in each table are related to internal loss factors. The lines correspond to internal loss factor 1 whereas the columns yield values for internal loss factor 2. For a given doublets of loss factors, the value of the natural frequency ratio is found at the cross section between line and column. It is worth noting that the table is not exactly symmetric insofar as ω_1 does not change. Table 11 displays x_{min} and Table 12 gives x_{max}.

TABLE 11

Loss factor 1

Loss factor 2 \ Loss factor 1	0·1	0·09	0·08	0·07	0·06	0·05	0·04	0·03	0·02	0·01	0·009	0·008	0·007	0·006	0·005	0·004	0·003	0·002	0·001
0·1	0·753	0·753	0·753	0·753	0·753	0·753	0·753	0·814	0·876	0·907	0·923	0·938	0·938	0·938	0·954	0·949	0·941	0·938	0·999
0·09	0·753	0·753	0·753	0·753	0·753	0·753	0·753	0·768	0·814	0·907	0·907	0·938	0·938	0·938	0·954	0·951	0·943	0·938	0·999
0·08	0·783	0·753	0·753	0·753	0·753	0·753	0·753	0·768	0·814	0·907	0·907	0·938	0·938	0·938	0·954	0·953	0·947	0·969	0·999
0·07	0·783	0·753	0·753	0·753	0·753	0·753	0·753	0·783	0·814	0·907	0·907	0·923	0·938	0·938	0·954	0·955	0·949	0·969	0·999
0·06	0·783	0·783	0·753	0·753	0·753	0·753	0·753	0.783	0.814	0·907	0·907	0·923	0·938	0·938	0·954	0·956	0·953	0·969	0·999
0·05	0·783	0·783	0·753	0·753	0·753	0·753	0·753	0·783	0·814	0·907	0·907	0·907	0·938	0·938	0·954	0·957	0·956	0·969	0·992
0·04	0·753	0·783	0·783	0·753	0·753	0·753	0·753	0·814	0·814	0·892	0·907	0·907	0·938	0·938	0·938	0·954	0·958	0·969	0·992
0·03	0·814	0·814	0·783	0·753	0·814	0·783	0·753	0·814	0·814	0·892	0·892	0·907	9·907	0·938	0·938	0·954	0·960	0·969	0·992
0·02	0·814	0·845	0·814	0·845	0·814	0·814	0·845	0·814	0·814	0·876	0·876	0·907	0·907	0·907	0·938	0·954	0·961	0·965	0·984
0·01	0·907	0·907	0·907	0·907	0·907	0·907	0·907	0·876	0·876	0·907	0·907	0·907	0·907	0·907	0·938	0·938	0·954	0·962	0·977
0·009	0·923	0·923	0·923	0·907	0·907	0·907	0·907	0·892	0·892	0·907	0·907	0·907	0·907	0·938	0·938	0·938	0·954	0·962	0·977
0·008	0·938	0·938	0·938	0·938	0·923	0·923	0·923	0·907	0·907	0·907	0·907	0·907	0·923	0·923	0·938	0·938	0·954	0·962	0·977
0·007	0·938	0·938	0·938	0·938	0·938	0·938	0·938	0·907	0·907	0·907	0·923	0·923	0·923	0·938	0·938	0·954	0·954	0·962	0·977
0·006	0·938	0·938	0·938	0·938	0·938	0·938	0·938	0·938	0·923	0·923	0·923	0·938	0·938	0·938	0·938	0·954	0·961	0·962	0·977
0·005	0·950	0·950	0·950	0·954	0·954	0·954	0·954	0·938	0·938	0·938	0·938	0·938	0·938	0·938	0·954	0·954	0·961	0·962	0·977
0·004	0·943	0·945	0·949	0·951	0·955	0·956	0·957	0·954	0·954	0·938	0·954	0·954	0·954	0·954	0·954	0·954	0·962	0·963	0·977
0·003	0·935	0·939	0·943	0·947	0·951	0·955	0·958	0·960	0·961	0·961	0·961	0·961	0·961	0·961	0·961	0·962	0·962	0·965	0·977
0·002	0·938	0·938	0·938	0·969	0·969	0·969	0·969	0·969	0·961	0·963	0·963	0·962	0·962	0·962	0·963	0·963	0·965	0·969	0·977
0·001	0·999	0·999	0·999	0·999	0·999	0·992	0·992	0·992	0·985	0·977	0·977	0·977	0·977	0·977	0·977	0·977	0·977	0·977	0·984

TABLE 12

Loss factor 1

Loss factor 2	0·1	0·09	0·08	0·07	0·06	0·05	0·04	0·03	0·02	0·01	0·009	0·008	0·007	0·006	0·005	0·004	0·003	0·002	0·001
0·1	1·250	1·250	1·250	1·250	1·375	1·375	1·250	1·250	1·188	1·094	1·094	1·063	1·063	1·063	1·055	1·060	1·069	1·063	1·001
0·09	1·250	1·250	1·250	1·250	1·250	1·250	1·250	1·250	1·188	1·094	1·094	1·063	1·063	1·063	1·055	1·058	1·065	1·063	1·001
0·08	1·375	1·375	1·250	1·250	1·250	1·250	1·250	1·250	1·188	1·094	1·094	1·063	1·063	1·063	1·055	1·054	1·062	1·063	1·001
0·07	1·375	1·250	1·250	1·375	1·375	1·375	1·250	1·250	1·188	1·094	1·094	1·094	1·063	1·063	1·047	1·048	1·058	1·031	1·001
0·06	1·375	1·375	1·375	1·250	1·250	1·250	1·250	1·250	1·250	1·125	1·094	1·094	1·063	1·063	1·047	1·046	1·048	1·031	1·008
0·05	1·313	1·313	1·313	1·375	1·250	1·250	1·250	1·250	1·188	1·125	1·094	1·094	1·063	1·063	1·047	1·046	1·044	1·031	1·008
0·04	1·250	1·250	1·313	1·313	1·313	1·313	1·313	1·250	1·188	1·125	1·094	1·094	1·078	1·063	1·063	1·047	1·044	1·031	1·008
0·03	1·297	1·297	1·297	1·313	1·250	1·250	1·250	1·250	1·250	1·125	1·125	1·094	1·078	1·063	1·063	1·047	1·042	1·031	1·008
0·02	1·250	1·250	1·250	1·250	1·250	1·250	1·250	1·250	1·188	1·125	1·125	1·094	1·094	1·078	1·063	1·047	1·041	1·039	1·016
0·01	1·094	1·094	1·125	1·125	1·125	1·125	1·125	1·125	1·125	1·125	1·125	1·094	1·094	1·078	1·063	1·063	1·047	1·039	1·023
0·009	1·094	1·094	1·094	1·094	1·094	1·125	1·125	1·125	1·125	1·102	1·094	1·094	1·094	1·078	1·063	1·063	1·047	1·039	1·023
0·008	1·063	1·063	1·063	1·094	1·094	1·094	1·094	1·125	1·125	1·094	1·094	1·094	1·094	1·078	1·063	1·063	1·047	1·039	1·023
0·007	1·063	1·063	1·063	1·063	1·078	1·063	1·094	1·094	1·094	1·094	1·094	1·094	1·094	1·063	1·063	1·047	1·039	1·039	1·023
0·006	1·063	1·063	1·063	1·063	1·063	1·063	1·063	1·063	1·094	1·094	1·094	1·078	1·078	1·0673	1·063	1·047	1·043	1·039	1·023
0·005	1·055	1·047	1·047	1·047	1·063	1·047	1·063	1·063	1·063	1·070	1·063	1·063	1·063	1·063	1·063	1·047	1·043	1·039	1·023
0·004	1·056	1·054	1·050	1·048	1·046	1·047	1·047	1·047	1·063	1·063	1·063	1·063	1·063	1·047	1·047	1·047	1·043	1·039	1·023
0·003	1·063	1·060	1·056	1·054	1·050	1·046	1·044	1·040	1·041	1·047	1·047	1·047	1·047	0·047	1·043	1·043	1·040	1·039	1·023
0·002	1·063	1·063	1·063	1·031	1·031	1·031	1·031	1·039	1·039	1·039	1·039	1·040	1·040	1·040	1·039	1·039	1·039	1·031	1·023
0·001	1·001	1·001	1·001	1·001	1·001	1·008	1·008	1·008	1·016	1·023	1·023	1·023	1·023	1·023	1·023	1·023	1·023	1·023	1·016